TRANSVERSE 'MONOPOLE' INSTABILITY DRIVEN BY AN ELECTRON CLOUD?

E. Benedetto, D. Schulte, F. Zimmermann, CERN, Geneva, Switzerland; K. Ohmi, KEK, Japan;
Y. Papaphilippou, ESRF Grenoble, France; G. Rumolo, GSI Darmstadt, Germany

Abstract

We simulate the long-term emittance growth of a proton beam due to an electron cloud of moderate density. This emittance growth is sometimes characterized by a rapid blow up of the bunch tail, and it appears to be different from the strong head-tail instability, which is observed at higher electron densities. We study whether this instability can occur in the absence of transverse dipole motion along the bunch, and its sensitivity to various simulation parameters, such as the number of beam-electron interaction points (IPs) and the phase advances between them. Using a frozen-potential model, we compute tune footprints, which reveal the resonances contributing to the incoherent part of the emittance growth.

1 INTRODUCTION

A beam blow up and vertical instability caused by an electron cloud in the KEK B factory and in the CERN SPS have been explained by a mechanism similar to the strong head-tail (or TMCI) instability [1]. However, at the PEP-II B factory the beam already blows up below the 'TMCI' threshold. A similar phenomenon was seen in simulations by Cai [2]. At EPAC 2002, Lotov and Stupakov reported a new type of 'monopole' instability for PEP-II, that occurs in the absence of any dipole motion and is characterized by a fast blow up of the bunch tail [3].

Recent simulations of the beam-electron interaction for the LHC proton beam using the codes HEADTAIL [4] and PEHTS [5] indicate a significant long-term emittance growth, already at low electron densities [6, 7]. Since the LHC beam has to be stored for several hours, even a few percent emittance growth over one hour can be a concern. The emittance increase observed in our simulation could be related to that observed by Cai or Lotov and Stupakov. Below we present the results of a simulation campaign which explored the nature of the emittance growth.

2 SIMULATIONS

Throughout this paper, we discuss only the effect of the electron cloud, and do not take into account additional space-charge forces or conventional impedances. The simulation parameters are those listed in Table 1, unless noted otherwise. In the simulation, the proton beam and the electron cloud interact at a few discrete 'interaction points' (IPs) around the ring, where we compute the integrated effect of a large number of electrons, which in reality are spread out over a long section of the ring. The implicit assumption is that the electrons introduce only a small perturbation.

Figure 1 shows simulations using the HEADTAIL code [4] for the LHC, where we consider a single IP per turn. The various curves refer to different average electron-cloud densities. The growth rates are significant for most of the cases. The saturation after a ten- or twenty-fold increase in emittance is due to the finite size of the grid used in the simulation, which here extends over $\pm 10\sigma$ (± 8.84 mm). Figure 2 compares results from HEADTAIL and PEHTS for different cloud sizes. The curves obtained from the two codes are similar.

Table 1: Simulation parameters, representing an electron cloud at injection into the LHC.

parameter	symbol	value
electron cloud density	ρ_e	6×10^{11} m^{-3}
bunch population	N_b	1.1×10^{11}
beta function	$\beta_{x,y}$	100 m
rms bunch length	σ_z	0.115 m
rms beam size	$\sigma_{x,y}$	0.884 mm
rms momentum spread	$\delta_{\rm rms}$	4.68×10^{-4}
synchrotron tune	Q_s	0.0059
momentum compaction	α_c	3.47×10^{-4}
circumference	C	26.659 km
nominal tunes	$Q_{x,y}$	64.28, 59.31
chromaticity	$Q'_{x,y}$	2, 2
relativistic factor	γ	479.6

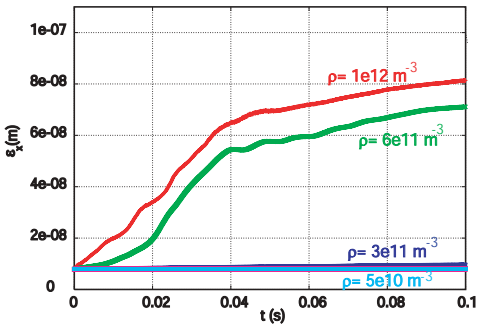

Figure 1: Evolution of LHC emittance vs. time in seconds for an LHC bunch at injection simulated by HEADTAIL for different densities.

Simulations in Fig. 3 illustrate the stabilizing effect of increasing the synchrotron tune Q_s. Above a threshold value for Q_s, the sudden large emittance growth disappears and only a continuous much smaller growth remains. This transition is the threshold of the TMCI instability. However, even the much reduced growth below the TMCI threshold could dilute the LHC proton beam. Comparing the two pictures we observe that for a two times increased electron density the threshold synchrotron tune is also two times larger, consistent with the TMCI model of [1].

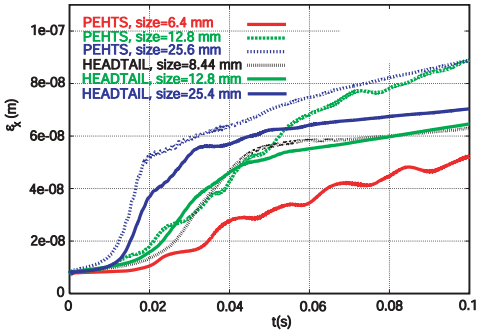

Figure 2: Comparison of HEADTAIL and PEHTS results for various grid sizes, considering a single IP.

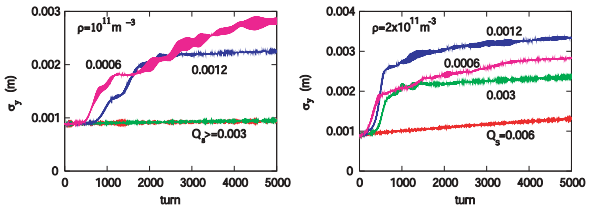

Figure 3: Evolution of LHC vertical beam size vs. time in turns, simulated by the code PEHTS for $\rho_e = 10^{11}$ m^{-3} (left) and $\rho_e = 2 \times 10^{11}$ m^{-3} (right). The curves correspond to different synchrotron tunes as indicated.

From basic considerations, for a constant ratio of density and synchrotron tune, the emittance growth should look similar, if we scale the time axis with the density (or with Q_s). Figure 4 illustrates that this scaling is nearly fulfilled.

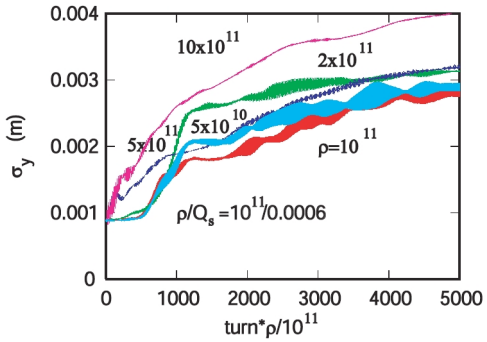

Figure 4: Evolution of LHC vertical beam size vs. the normalized product of turns and electron density, simulated by PEHTS for different densities and synchrotron tunes, keeping a constant ratio ρ_e/Q_s.

Repeating the simulation of Fig. 1 for different numbers of IPs, we obtain the results in picture (a) of Fig. 5. By increasing the number of IPs from 1 to 5 (and above), we do not observe any clear convergence of the simulated emittance evolution, but instead we find a rather erratic and non-monotonic dependence. A tentative explanation is that, as we increase the number of IPs and distribute them uniformly around the ring, the phase advance between successive IPs changes abruptly, and for different numbers of IPs the beam experiences resonances of unequal strength.

Figure 6 compares snap shots of the slice centroids and

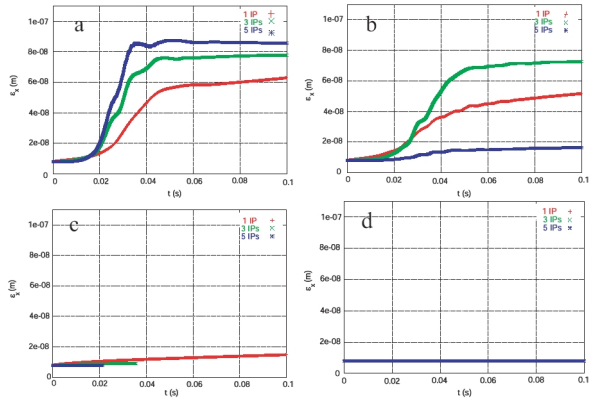

Figure 5: Simulated evolution of LHC emittance vs. time in seconds for $\rho_e = 6 \times 10^{11}$ m^{-3}; the curves correspond to different numbers of IPs. (a) full simulation with fixed phase advances between IPs; (b) bunch centroid motion suppressed at each IP; (c) bunch-slice centroid motion suppressed; (d) perfect symmetrization of beam and electron macro-particles.

the local beam size after 20 and 40 ms in simulations with 1 and 5 IPs. For the case of a single IP, there is less motion along the bunch. In the vertical plane (not shown), the behaviour for 1 IP is different, and all bunch slices blow up steadily starting from time zero. A possible interpretation is that for 1 IP the stronger nonlinear forces and the larger tune spread induced by the electrons during the bunch passage lead to a more rapid filamentation than for 5 IPs.

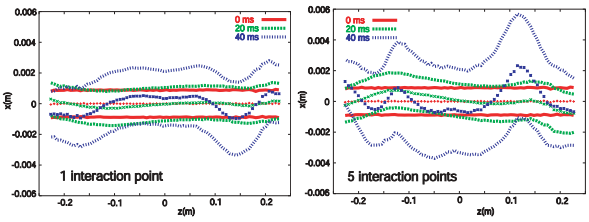

Figure 6: Simulated horizontal bunch shape (centroid and rms beam size) after 0, 20 ms, and 40 ms in the LHC, assuming an electron density of $\rho_e = 6 \times 10^{11}$ m^{-3} and either 1 (left) or 5 (right) beam-cloud interactions per turn.

In order to better reveal the character of the instability, the simulation was modified, by (1) removing the bunch centroid oscillation once per IP, (2) removing the centroid of each longitudinal bunch slice once per IP, and (3) completely symmetrizing the initial distribution of macroparticles representing beam and electrons, so that for each particle at position (x, y) there are equivalent partners at $(x, -y)$,$(-x, y)$, and $(-x, -y)$. In this way, any dipole motion is completely removed. The results of these three changes are illustrated in pictures b–d of Fig. 5. Suppressing the centroid bunch motion reduces the emittance growth, but does not eliminate it. Removing the slice centroids is much more efficient, but a small emittance growth remains, especially for 1 IP. Symmetrization fully removes any emittance growth. This rules out the existence of a pure monopole instability, for the parameters considered.

To reduce the sensitivity to resonances in the original model including full dipolar motion, we have introduced a random phase advance between successive IPs, always maintaining the correct average tune. The result is shown in the left picture of Fig. 7. The simulated emittance growth now monotonically approaches smaller values as the number of IPs is increased. For few IPs, the overall level of the emittance growth is higher than in the case of constant phase advance (compare the top left picture of Fig. 5). The larger growth is probably due to noise from the randomization. Plotting the initial linear growth rate as a function of IP number, we observe an inversely linear dependence, which suggests that the emittance growth may approach zero in the limit of infinitely many IPs.

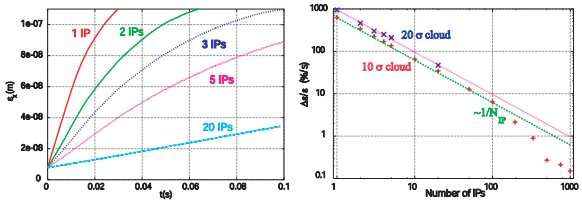

Figure 7: Left: simulated evolution of LHC emittance vs. time in seconds for $\rho_e = 6 \times 10^{11}$ m^{-3} with a random phase advances between IPs; the different curves correspond to different numbers of interaction points as indicated. Right: initial linear growth rate in the left plot as a function of the number of IPs; a $1/N$ dependence is superimposed.

In the usual multi-particle simulation the motion of individual protons is not governed by a Hamiltonian. We constructed a Hamiltonian system as follows. First, we computed the electric field of the electrons during a single bunch passage, we stored these values for each time step of the bunch passage, and next, in a separate simulation, we applied these stored fields at either 1 or 5 IPs per turn to simulate the motion of protons over a few thousand turns. For this frozen field, the simulated emittance growth was much smaller than for the complete simulations above. This confirms that the emittance growth is mainly a dynamic effect due to a (dipolar) two-stream instability, and it also demonstrates that diffusive single-particle motion is of secondary importance.

Figure 8 shows a tune footprint obtained from the corresponding frequency-map analysis for a case when the synchrotron motion was switched off (synchrotron motion adds an additional degree of freedom, making it difficult to determine the fundamental frequencies). For 1 IP, there is a multitude of excited resonances, with most importantly the $(0,3)$, $(1,-4)$ and some of higher order (especially 10th). By contrast, the 5-IP case does not show any resonance excitation. A similar resonant behaviour appears in the equivalent 6-dimensional simulation (not shown), but here the synchrotron motion is obscuring the picture. The line of points formed in the left corner of the two diagrams is not a resonance, but reflects particles far ahead or behind the bunch, which do not interact with the electron cloud. It is an artifact of our simulation.

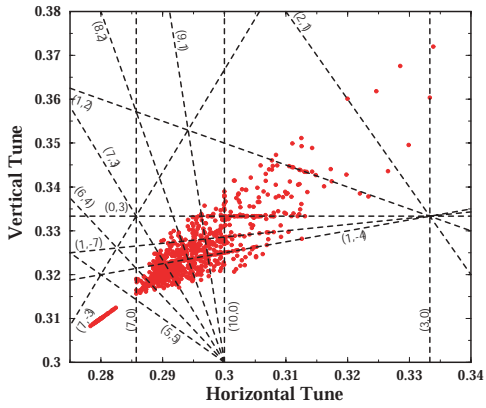

Figure 8: Tune footprint obtained from tracking through a frozen electron potential with 1 IP per turn by a frequency-map analysis [8].

The tune shift expected from the unperturbed cloud is [9] $\Delta Q_{x,y} \approx r_p/(2\gamma)\beta_{x,y}\rho_e C$, which amounts to about 0.003 in our example, The spread of the tune footprints in Fig. 8 is about 20 times larger, evidence of the highly nonlinear field of the electron cloud during a bunch passage.

3 CONCLUSIONS

A slow long-term emittance growth caused by an electron cloud of low density could be important for proton storage rings like the LHC. Our simulations show that the emittance growth observed in the simulations is not due to a monopole instability. It depends strongly on the number of interaction points and on the inter-IP phase advances. Nonlinear resonances, of order 3–10, can be excited by the field of the electron cloud and may also contribute to the emittance growth. Preliminary results for a random phase advance suggest that below the TMCI threshold the simulated emittance growth converges towards zero, as the number of IPs is increased. In the future, we plan to calibrate our simulation against the code QUICKPIC [10], which models a continuous electron cloud instead of discrete IPs.

We thank A. Ghalam, T. Katsouleas and F. Ruggiero for helpful discussions.

4 REFERENCES

[1] K. Ohmi, F. Zimmermann, PRL 85, p. 3821 (2000).

[2] Y. Cai, ECLOUD'02, CERN-2002-001, p. 141 (2002).

[3] K.V. Lotov, G.V. Stupakov, EPAC 2002, Paris, p. 1643.

[4] G. Rumolo et al., ECLOUD'02, CERN-2002-001, 147.

[5] K. Ohmi, Proc. PAC2001, Chicago, p. 1895 (2001).

[6] E. Benedetto et al., Chamonix'03, CERN-AB-2003-008.

[7] G. Arduini et al., "Present Understanding of Electron Cloud Effects in the Large Hadron Collider," these proceedings.

[8] J. Laskar, Astron. Astrophys. 198, 341 (1988).

[9] K. Ohmi et al., Proc. APAC'01, p. 445 (2001).

[10] G. Rumolo, A. Ghalam, T. Katsouleas et al., to be published.